27th EPS Conference on Contr. Fusion and Plasma Phys. Budapest, 12-16 June 2000 ECA Vol. **24B** (2000) 608 -611

Multi-Mode Model Transport Simulations of Internal Transport Barriers in JET and DIII-D*

Arnold H. Kritz,† P. Zhu,‡ G. Bateman,† and W. Horton‡

† *Physics Department, Lehigh University, Bethlehem, PA 18015*
‡ *Institute for Fusion Studies, The University of Texas at Austin, Austin, Texas 78712*

Predictive simulations are shown to reproduce the onset and time evolution of internal transport barriers in high performance JET and DIII-D discharges. The JET discharge is particularly complex: The simulation follows the transition from Ohmic to L-mode, to the formation of an internal transport barrier, to the transition to H-mode (implemented as a time-dependent boundary condition in the simulation), and then to the subsequent motion of the internal transport barrier. The timing and location of the internal transport barrier in the simulations are in good agreement with the experimental data, particularly for the DIII-D discharge considered. The internal transport barrier results from combined effects of $\mathbf{E} \times \mathbf{B}$ flow shear and weak magnetic shear in these simulations.

Internal Transport Barriers (ITBs) have now been observed in most large tokamaks. An ITB is a narrow region in the plasma core characterized by a steep temperature and/or density gradient. It has been found that the toroidal rotation velocity gradient is steep in a region within the ITB and that ITBs can occur with a lower power threshold than required for the high confinement mode (H-mode) regime, where the transport barrier is located at the plasma edge.

Results are presented here for simulations carried out for a JET optimized shear discharge, 40542, and a DIII-D negative central shear discharge, 84682, using the time-dependent 1-1/2-D BALDUR transport code where sources and sinks are computed self-consistently. The Multi-Mode transport model [1] used in this study is modified using either the Hahm-Burrell [2] or the Hamaguchi-Horton [3] flow shear stabilization mechanism.

The Multi-Mode model determines multiple channel anomalous transport coefficients by combining transport contributions from several modes that co-exist in tokamak plasmas. These include ion temperature gradient (ITG) and trapped electron modes (TEM) in the quasilinear Weiland model [4, 5], the drift-Alfvén modes in a model developed by Scott and Bateman [6, 7], as well as an empirical model for kinetic ballooning modes. Note, in the version of Multi-Mode model used in this paper, we replace the MMM95 resistive ballooning mode model at plasma edge with the drift-Alfvén mode model [7].

The $\mathbf{E} \times \mathbf{B}$ flow shear mechanism is implemented in the current version of the Multi-Mode model either by subtracting the Hahm-Burrell shearing rate, ω_s, from the drift mode growth rate [2], or by multiplying the ion drift mode induced transport coefficients by the Hamaguchi-Horton suppression factor $1/(1+(\Upsilon_s/\Upsilon_{sc})^2)$ [3], where ω_s and Υ_s, are

*Supported by U.S. DOE contracts DE-FG02-92-ER-5414 and DE-FG03-96ER-54346.

defined by

$$\omega_s \equiv \left| \frac{RB_\theta}{B_\phi} \frac{\partial}{\partial r} \left(\frac{E_r}{RB_\theta} \right) \right| \qquad \text{and} \qquad \Upsilon_s \equiv \sqrt{\frac{m_i}{T_e}} \left| \frac{R\partial_\psi (E_r/RB_\theta)}{\partial_\psi \ln q} \right| .$$

and Υ_{sc} is the critical value ($\Upsilon_{sc} \simeq 1$). Here, R is the plasma major radius; B_θ and B_ϕ, the toroidal and poloidal magnetic fields; m_i, the ion mass; T_e, the electron temperature; and ψ is the magnetic stream function. Both ω_s and Υ_s are computed using the radial electric field E_r, which is computed from the poloidal and toroidal flow velocities and the pressure gradient. The poloidal flow velocity is computed using a neoclassical model [8], while the toroidal flow velocity is taken from the experimental data.

The magnetic shear effect enters the Weiland model for drift modes through its influence on the form of the perturbations along the magnetic field lines [4]. In regions of strong magnetic shear, the electron motions parallel to the magnetic field line are greatly impeded; hence, the perturbations are strongly ballooning-like. This ballooning feature of the perturbation and the growth rate of the mode are reduced in regions of weak magnetic shear. This mechanism is implemented in Weiland model through the averaged ion acoustic operator $< \nabla_\parallel^2 >$ and the averaged Alfvén operator $< \nabla_\parallel \nabla_\perp^2 \nabla_\parallel >$, which are reduced where magnetic shear is weak.

Results are compared in simulations with and without the Hahm-Burrell or Hamaguchi-Horton flow shear mechanisms included in the model. With the flow shear mechanisms included, good agreement between the simulations and the experimental data was obtained. The relative rms deviations between simulation profiles of temperature and density and experimental data are less than 20% for all auxiliary heated time stages of the JET discharges. In the DIII-D discharges, the overall rms deviations are significantly smaller. The formation and radial movement of internal transport barriers are interpreted as resulting from a combination of $\mathbf{E} \times \mathbf{B}$ flow shear and weak magnetic shear mechanisms.

The experimental and simulation ion temperature profiles at six time slices are shown in Fig. 1 for one of the JET discharges and for one of the DIII-D discharges. In the simulations shown in Fig. 1, the Hahm-Burrell model is employed. We use the TRANSP processed experimental data from the International Profile database for the comparison with the simulations.

The JET simulation starts during the ohmic stage and proceeds until the end of all auxiliary heating. The first time slice for the JET discharges is the in the middle of ohmic stage, and the second time slice is right before the auxiliary heating is turned on. The third and fourth time slice are taken right after the internal transport barrier forms and just before the formation of the edge transport barrier. The last two time slices are during the stage when the internal transport barrier co-exists with the ELMy H-mode at the edge and before the time when the NBI heating is turned down.

The DIII-D simulation starts at the beginning of the neutral beam heating stage, where the experimental data is available. The heating starts with a lower power, and steps up to about double power in the middle of the shot. Plots of the ion temperature profiles at two time slices before, one time slice during, and three time slices after the neutral beam power step-up are presented. The timing and location of the ITBs in the simulations agree well with the experimental data for discharges considered. For both the JET and

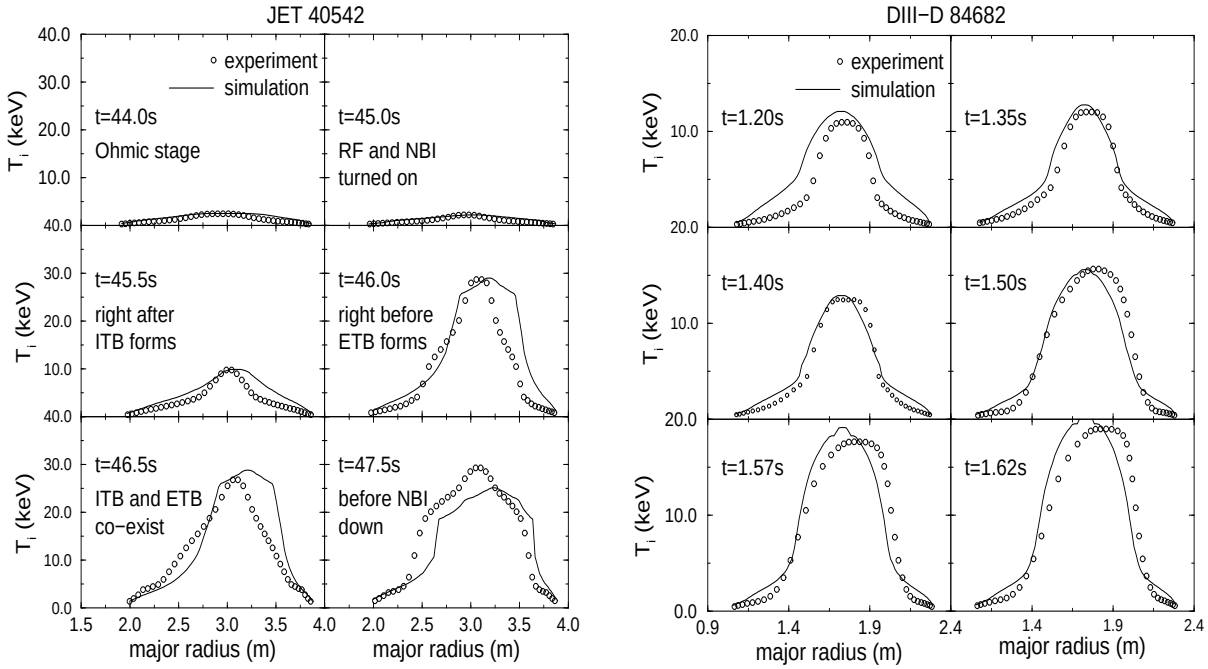

Figure 1: *Experimental ion temperature profiles as a function of major radius (open circles) and the corresponding optimized simulation profiles with Hahm-Burrell flow shear stabilization (solid curves) at six time slices for JET shot 40542, and DIII-D shot 84682.*

DIII-D discharges considered, the Hahm-Burrell and the Hamaguchi-Horton flow shear stabilization mechanism resulted in similar agreement between simulation and data.

The time evolution of the ion temperature profile for the JET discharge is shown in Figure 2. The curves in this figure show the ion temperature at equally spaced intervals in normalized minor radius as a function of time. The curve at the top is the ion temperature trace near the magnetic axis, while the curve at the bottom is the ion temperature trace at the edge of the plasma. The rest of the time traces are at equally spaced intervals of normalized minor radius. Internal transport barriers are characterized by wider spacing between adjacent curves (steeper gradients). It can be seen in Figure 2 that for both the experiment (left) and simulation (right), an internal transport barrier forms near the magnetic axis (close to top curve) and then moves closer to the edge of the plasma (lower curves). The simulation presented here uses the Multi-Mode model with Hahm-Burrell flow shear stabilization of the Weiland model.

It is seen in the experimental data in Fig. 2 that the ITB at t=46.0 s is near the central region (where the ion temperature increases from 20 to 28 keV). However, by t=47.5 s, the ITB has moved to a region closer to the plasma edge (where the ion temperature increase is 5 to 17 keV). In the simulation results there is a similar motion of the ITB. The ITB at t=46.0 s is near the central region of the plasma (where the ion temperature increases from 10 to 27 keV) while at t=47.5 s moved near to the edge where ITB is indicated by a temperature increase of 9 to 18 keV. Hence, both the experimental data the simulation shown in Fig. 2 indicated the trend of the outward radial movement of the ITB. The experimental data indicates that the region of large toroidal velocity gradient moves outward in radius between 46 and 47 seconds. In the corresponding simulation, it is found that the contribution to the radial electric field of the gradient in toroidal velocity

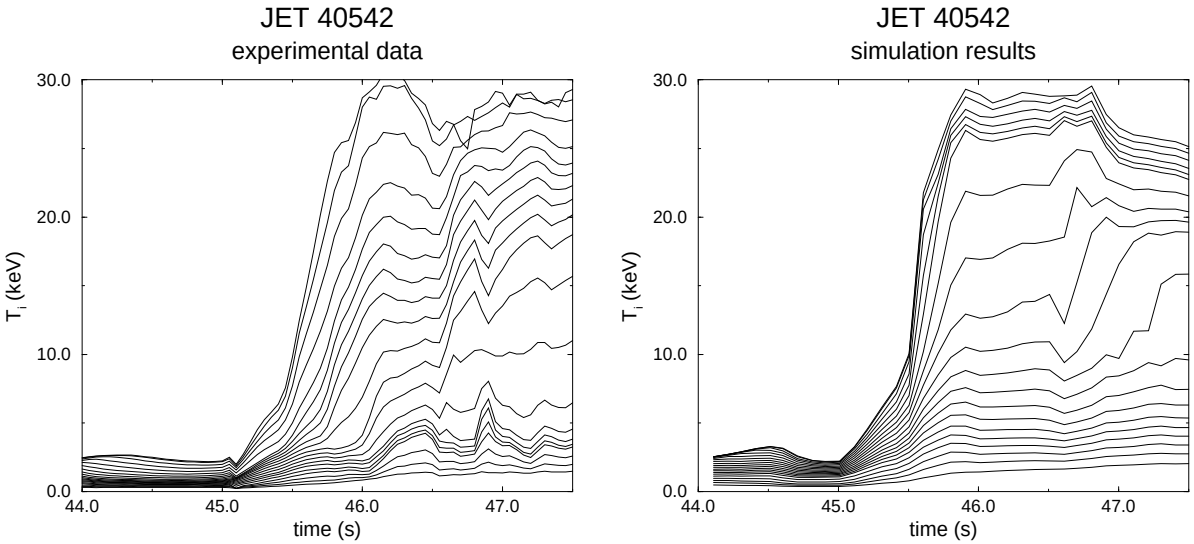

Figure 2: *Ion temperature as function of time at equally spaced intervals in normalized minor radius in experiment (left) and simulation (right) for JET discharge 40542.*

times poloidal magnetic field has a significant effect on the flow shear stabilization.

In the Multi-Mode model that we used here, the overall mechanisms of the ITB dynamics are implemented in three different levels: theoretical, empirical, and experimental. The theoretical models include the Weiland model for ion drift modes, the Scott and Bateman model for drift-Alfvén mode at plasma edge, and the neoclassical model for the poloidal plasma flow. The kinetic ballooning mode model and the $\mathbf{E} \times \mathbf{B}$ flow shear mechanism are implemented empirically.

Simulations carried out with this transport model have reproduced the internal transport barriers observed in both JET and DIII-D discharges. We interpret the formation of internal transport barrier as resulting from the combined effects of $\mathbf{E} \times \mathbf{B}$ flow shear and the weak magnetic shear configuration. We considered two implementations of $\mathbf{E} \times \mathbf{B}$ flow shear mechanism: 1) ion drift mode growth rate is reduced by Hahm-Burrell $\mathbf{E} \times \mathbf{B}$ flow shearing rate and 2) ion drift mode induced transport coefficients are reduced by the Hamaguchi-Horton shear suppression factor. For the simulations presented, and for additional discharges studied [9], these two methods yield similar results.

[1] G.Bateman, A.Kritz, J.Kinsey, A.Redd and J.Weiland, Phys. Plasmas **5**, 1793 (1998).
[2] T. S. Hahm and K. H. Burrell, Phys. Plasmas **2**, 1648 (1995).
[3] S. Hamaguchi and W. Horton, Phys. Fluids B **4**, 319 (1992).
[4] J. Weiland and A. Hirose, Nuclear Fusion **32**, 151 (1992).
[5] J. Nilsson and J. Weiland, Nuclear Fusion **34**, 803 (1994).
[6] B. Scott, Plasma Phys. and Controlled Fusion bf 39, 1635 (1997).
[7] G. Bateman, A. H. Kritz, A. J. Redd, M. Erba, G. Rewoldt, J. Weiland, P. Strand, J. E. Kinsey, and B. Scott, in *Proceedings of the Seventeenth IAEA Conference, (Yokahama, Japan, 1988)* (IAEA, Vienna, 1999), paper IAEA-F1-CN-69/THP2-19.
[8] P. Zhu, W. Horton, and H. Sugama, Phys. Plasmas **6**, 2503 (1999).
[9] P. Zhu, G. Bateman, A. Kritz and W. Horton, *Predictive transport simulations of internal transport barriers using the multi-mode model*, to appear Phys. Plasmas, July (2000).